

A Normal-Gamma Dirichlet Process Mixture Model

Dawei Ding*, George Karabatsos

University of Illinois-Chicago, United States

Abstract

We propose a Dirichlet process mixture (DPM) for prediction and cluster-wise variable selection, based on a Normal-Gamma baseline distribution on the linear regression coefficients, and which gives rise to strong posterior consistency. A simulation study and real data application showed that in terms of predictive and variable selection accuracy, the model tended to outperform the standard DPM model assigned a normal prior with no variable selection. Software code is provided in the Supplementary Information.

Keywords: Bayesian nonparametrics, Clustering, Regression, Variable selection

1. Introduction

For linear regression with variable (covariate) selection, the LASSO is a prominent method with many extensions (Tibshirani, 1996, 2011). This method employs a shrinkage parameter which for sufficiently large values can shrink the coefficients of irrelevant covariates to zero, and is the inverse scale parameter of independent zero-mean Laplace prior distributions on the coefficients. Park and Casella (2008) considered a fully Bayesian LASSO by exploiting the representation of the Laplace prior as a scale mixture of zero-mean normal distributions with exponential mixing density (Andrews and Mallows, 1974). Griffin and Brown (2010) generalized this to a Normal-Gamma prior distribution, which induces adaptive shrinkage and has thicker tails, and in turn shrinks less on larger coefficients while sufficiently shrinking smaller ones. Such an absolutely continuous shrinkage prior is advantageous to spike-and-slab priors for variable selection, which require high computational cost to search through a large number of possible submodels for many covariates (Castillo et al., 2015).

One key limitation of existing priors is they do not allow variable selection to vary over different clusters of the data points. However, few methods addressed this problem. Barcella et al. (2016) proposed a covariate-dependent Dirichlet Process Mixture (DPM) model which assigns a spike-and-slab prior distribution to achieve cluster-wise variable selection for binary covariates. Quintana et al. (2015) proposed cluster-wise variable selection in a product partition model by employing binary indicator parameters on the covariate similarity function. Meanwhile, DPM modeling of both covariate and conditional response distributions, the *joint DPM* modeling approach (Wade et al., 2014b), can provide better

*Corresponding author

Email address: dding20@uic.edu (Dawei Ding)

predictive accuracy than DPM modeling which assumes fixed covariates, because it accounts for the distance between a new covariate profile \mathbf{x} and the data-observed \mathbf{x} values of the different cluster groups (Hannah et al., 2011).

We propose a novel DPM of regressions model which assigns a Normal-Gamma shrinkage prior on the regression coefficients, to provide prediction and cluster-wise variable selection. The model is based on the Dependent Dirichlet Process (DDP), a wide and flexible class of covariate-dependent random probability measures (MacEachern, 1999; Quintana et al., 2020).

Next, Section 2 further describes our proposed DPM model. It also characterizes its posterior and posterior predictive distributions, provides a corresponding MCMC algorithm for the model, and proves the strong consistency of the model’s posterior distribution. Finally, this section also reviews methods for summarizing the MCMC posterior sample output for variable selection and clustering estimation. Section 3 compares our DPM model against the standard DPM model which assigns a normal prior with no variable selection, in terms of predictive, variable selection, and clustering accuracy. Section 4 illustrates our DPM model on a real data set. Section 5 concludes the article.

2. Model and Posterior Inference

2.1. Normal-Gamma DPM Model (NG-DPM)

Given a data set matrix $(\mathbf{y}, \mathbf{X}) = (y_i, \mathbf{x}_i^T)_{i=1}^n$ including n observations of $p \times 1$ covariate vectors \mathbf{x}_i and scalar responses y_i , our DPM model is the mixture of Normal (N) probability densities:

$$(y_i, \mathbf{x}_i) | G \stackrel{iid}{\sim} \int N(y | \mu + \mathbf{x}^T \boldsymbol{\beta}, \sigma^2) N_p(\mathbf{x} | \mathbf{m}, \text{diag}(\boldsymbol{\tau})) G(d(\boldsymbol{\theta})), \quad (1)$$

for $i = 1, \dots, n$, where $\boldsymbol{\theta} = \{\boldsymbol{\theta}_y, \boldsymbol{\theta}_x\}$, $\boldsymbol{\theta}_y = \{\mu, \boldsymbol{\beta}\}$, and $\boldsymbol{\theta}_x = \{\mathbf{m}, \boldsymbol{\tau}\}$, with mixing distribution $G \sim \text{DP}(\alpha, G_0)$ assigned a Dirichlet Process prior with mass parameter $\alpha > 0$ and baseline measure G_0 (Ferguson, 1973).

Since the support of the DP prior is almost surely discrete, the general mixture model (1) can also be expressed as the countable mixture:

$$f(y, \mathbf{x} | G) = \sum_{j=1}^{\infty} N(y | \mu_j + \mathbf{x}^T \boldsymbol{\beta}_j, \sigma^2) N_p(\mathbf{x} | \mathbf{m}_j, \text{diag}(\boldsymbol{\tau}_j)) w_j. \quad (2)$$

Specifically, the Dirichlet Process G in (1) admits the stick-breaking representation of infinite mixture $G(\cdot) = \sum_{j=1}^{\infty} w_j \delta_{\boldsymbol{\theta}_j}(\cdot)$, where $\boldsymbol{\theta}_j = \{\mu_j, \boldsymbol{\beta}_j, \mathbf{m}_j, \boldsymbol{\tau}_j\} \stackrel{iid}{\sim} G_0$, $\delta_{\boldsymbol{\theta}_j}$ is the Dirac measure that takes the value 1 on $\boldsymbol{\theta}_j$ and 0 elsewhere, and the mixing weights have the stick-breaking form $w_j = v_j \prod_{l=1}^{j-1} (1 - v_l)$ where $v_j \sim \text{Beta}(1, \alpha)$ for $j = 1, 2, \dots$, $\sum_{j=1}^{\infty} w_j = 1$ (Sethuraman, 1994).

The DPM mixture model (2) is completed by the specification of the following prior density functions for the model parameters, including the Normal-Gamma prior (Griffin and Brown,

2010) specified as the DP baseline measure G_0 :

$$g_0(\mu_j, \boldsymbol{\beta}_j, \mathbf{m}_j, \boldsymbol{\tau}_j) = \text{N}(\mu_j|0, \nu_\mu) \text{N}_p(\boldsymbol{\beta}_j|\mathbf{0}, \mathbf{D}_{\psi_j}) \quad (3a)$$

$$\times \prod_{l=1}^p \left[\text{N}(m_{lj}|m_0, \frac{\tau_{lj}}{n_0}) \text{Inv-Gamma}(\tau_{lj}|\frac{\nu_0}{2}, \frac{2}{\nu_0 s_0^2}) \right]$$

$$\mathbf{D}_{\psi_j} = \text{diag}(\psi_{1j}, \dots, \psi_{pj}) \equiv \text{diag}(\boldsymbol{\psi}_j), \quad j = 1, 2, \dots \quad (3b)$$

$$\pi(\boldsymbol{\psi}_j|\lambda_j, \gamma_j^{-2}) = \prod_{l=1}^p \text{Gamma}(\psi_{lj}|\lambda_j, \frac{1}{2}\gamma_j^{-2}), \quad j = 1, 2, \dots \quad (3c)$$

$$\pi(\lambda_j, \gamma_j^{-2}) = \text{Exp}(\lambda_j|1) \text{Gamma}(\gamma_j^{-2}|2, \frac{2V}{\lambda_j}), \quad j = 1, 2, \dots \quad (3d)$$

$$\pi(\mathbf{v}) = \prod_{j=1}^{\infty} \text{Beta}(v_j|1, \alpha) \quad (3e)$$

$$\pi(\alpha) = \text{Gamma}(\alpha|\alpha_\alpha, \theta_\alpha) \quad (3f)$$

$$\pi(\sigma^2) = \text{Inv-Gamma}(\sigma^2|\alpha_0, \theta_0), \quad (3g)$$

where $V = \frac{1}{p} \sum_{l=1}^p \hat{\beta}_l^2 \mathbf{1}(n \geq p+1) + \frac{1}{n} \sum_{l=1}^p \tilde{\beta}_l^2 \mathbf{1}(n < p+1)$, $(\hat{\mu}, \hat{\boldsymbol{\beta}}^T)^T = (\tilde{\mathbf{X}}^T \tilde{\mathbf{X}})^{-1} \tilde{\mathbf{X}}^T \mathbf{y}$ is the least squares estimate, $(\tilde{\mu}, \tilde{\boldsymbol{\beta}}^T)^T = \tilde{\mathbf{X}}^T (\tilde{\mathbf{X}} \tilde{\mathbf{X}}^T)^{-1} \mathbf{y}$ is the minimum norm least squares estimate, $\tilde{\mathbf{X}} = [\mathbf{1}_n, \mathbf{X}]$, and where g_0 is the pdf of the baseline measure G_0 . The joint prior density of all the model parameters $\boldsymbol{\Lambda}$ in (3) is denoted as $\pi(\boldsymbol{\Lambda})$.

The conditional density of Y in the joint mixture model (2) can be written as:

$$f(y|\mathbf{x}, G) = \sum_{j=1}^{\infty} \text{N}(y|\mu_j + \mathbf{x}^T \boldsymbol{\beta}_j, \sigma^2) w_j(\mathbf{x}),$$

with covariate dependent mixture weights $w_j(\mathbf{x}) = \frac{w_j \text{N}_p(\mathbf{x}|\mathbf{m}_j, \text{diag}(\boldsymbol{\tau}_j))}{\sum_{h=1}^{\infty} w_h \text{N}_p(\mathbf{x}|\mathbf{m}_h, \text{diag}(\boldsymbol{\tau}_h))}$, implying that the model is based on the Dependent Dirichlet Process (Quintana et al., 2020).

2.2. Posterior Computations

After introducing latent variables u_i and cluster membership indicators d_i for $i = 1, \dots, n$, to deal with the infinite dimensionality of the DPM model (2)-(3), it can be shown that the joint posterior distribution of all the model parameters $\boldsymbol{\Lambda}$ and $\{(u_i, d_i), i = 1, \dots, n\}$, is proportional to:

$$\prod_{i=1}^n \left[\mathbf{1}(u_i < w_{d_i}) \text{N}(y_i|\mu_{d_i} + \mathbf{x}_i^T \boldsymbol{\beta}_{d_i}, \sigma^2) \prod_{l=1}^p \text{N}(x_{il}|m_{d_i,l}, \tau_{d_i,l}) \right] \pi(\boldsymbol{\Lambda}) \quad (4)$$

where $d_i = j$ if observation pair (y_i, \mathbf{x}_i) belonging to j th cluster, for $j = 1, 2, \dots$. Posterior inference of the DPM model proceeds after marginalizing over the latent variables $\{u_i : i = 1, \dots, n\}$.

Posterior inference with the model can be undertaken using a Gibbs sampling algorithm for normal linear models assigned a Normal-Gamma prior (Griffin and Brown, 2010), embedded within a slice sampler for DPM regression models (Karabatsos and Walker, 2012). See Appendix A for details.

2.3. Posterior Predictive Inference

Prediction from the joint DPM model is based on a generalized Pólya urn scheme (Wade et al., 2014a), and is described as follows.

A partition of the n data points is denoted as $\rho_n = \{d_i\}_{i=1}^n$, comprised of K distinct clusters or values of the d_i . Denote the corresponding cluster sets and members as $C_j = \{i : d_i = j\}$ and $\mathbf{X}_j^* = \{\mathbf{x}_i : i \in C_j\}$, $\mathbf{y}_j^* = \{y_i : i \in C_j\}$, for $j = 1, \dots, K$. Then, based on a covariate-dependent Pólya urn scheme, the cluster label for a new subject d_{n+1} conditionally on its corresponding profile \mathbf{x} , current partition ρ_n , and observations \mathbf{X} , has distribution given by:

$$d_{n+1}|\mathbf{x}, \mathbf{X}, \rho_n \sim \frac{\alpha\pi_n}{b_0} f_{0,\mathbf{x}}(\mathbf{x}) \delta_{K+1}(\cdot) + \frac{1}{b_0} \sum_{j=1}^K \pi_n n_j f_{j,\mathbf{x}}(\mathbf{x}) \delta_j(\cdot), \quad (5)$$

where $\pi_n = \frac{1}{\alpha+n}$, $n_j = |C_j|$, $\sum_{j=1}^K n_j = n$, $b_0 = p(\mathbf{x}|\rho_n, \mathbf{X})$,

$$f_{0,\mathbf{x}}(\mathbf{x}) = \int p(\mathbf{x}|\boldsymbol{\theta}_{\mathbf{x}}) G_0(d\boldsymbol{\theta}_{\mathbf{x}}), \text{ and } f_{j,\mathbf{x}}(\mathbf{x}) = \int p(\mathbf{x}|\boldsymbol{\theta}_{\mathbf{x}}) p(\boldsymbol{\theta}_{\mathbf{x}}|\mathbf{X}_j^*) d\boldsymbol{\theta}_{\mathbf{x}}.$$

Thus, the cluster allocation probability distribution (5) depends on new \mathbf{x} and the covariate data \mathbf{X} . The more similar a new profile \mathbf{x} is to the existing \mathbf{x}_i 's in cluster j , the higher the density $p(\mathbf{x}|\boldsymbol{\theta}_{\mathbf{x}})$, leading to higher predictive density $f_{j,\mathbf{x}}(\mathbf{x})$, thus the higher probability of allocation to cluster j .

Once we obtain the allocation scheme for a new subject, we can then derive the conditional predictive density of the subject's response y , given her new profile \mathbf{x} and the data (\mathbf{y}, \mathbf{X}) , as:

$$\begin{aligned} & f(y|\mathbf{y}, \mathbf{X}, \mathbf{x}) \\ &= \sum_{\rho_n} \sum_{d_{n+1}} f(y|\mathbf{y}, \mathbf{X}, \mathbf{x}, \rho_n, d_{n+1}) p(d_{n+1}|\mathbf{X}, \mathbf{x}, \rho_n) p(\rho_n|\mathbf{y}, \mathbf{X}, \mathbf{x}) \\ &= \sum_{\rho_n} \left[\frac{\alpha\pi_n}{b_0} f_{0,\mathbf{x}}(\mathbf{x}) f_{0,y}(y|\mathbf{x}) + \frac{1}{b_0} \sum_{j=1}^K n_j \pi_n f_{j,\mathbf{x}}(\mathbf{x}) f_{j,y}(y|\mathbf{x}) \right] \frac{p(\mathbf{x}|\rho_n, \mathbf{X}) p(\rho_n|\mathbf{y}, \mathbf{X})}{p(\mathbf{x}|\mathbf{y}, \mathbf{X})} \\ &= \sum_{\rho_n} \left[\frac{\alpha\pi_n}{b_0} f_{0,\mathbf{x}}(\mathbf{x}) f_{0,y}(y|\mathbf{x}) + \frac{1}{b_0} \sum_{j=1}^K n_j \pi_n f_{j,\mathbf{x}}(\mathbf{x}) f_{j,y}(y|\mathbf{x}) \right] \frac{b_0 p(\rho_n|\mathbf{y}, \mathbf{X})}{p(\mathbf{x}|\mathbf{y}, \mathbf{X})} \\ &= \sum_{\rho_n} \left[\frac{\alpha\pi_n}{b} f_{0,\mathbf{x}}(\mathbf{x}) f_{0,y}(y|\mathbf{x}) + \frac{1}{b} \sum_{j=1}^K n_j \pi_n f_{j,\mathbf{x}}(\mathbf{x}) f_{j,y}(y|\mathbf{x}) \right] p(\rho_n|\mathbf{y}, \mathbf{X}) \\ &= \sum_{\rho_n} f(y|\mathbf{y}, \mathbf{X}, \mathbf{x}, \rho_n) p(\rho_n|\mathbf{y}, \mathbf{X}), \end{aligned}$$

where

$$b = p(\mathbf{x}|\mathbf{y}, \mathbf{X}), \quad f_{0,y}(y|\mathbf{x}) = \int p(y|\mathbf{x}, \boldsymbol{\theta}_y) G_0(\boldsymbol{\theta}_y), \quad f_{j,y}(y|\mathbf{x}) = \int p(y|\mathbf{x}, \boldsymbol{\theta}_y) p(\boldsymbol{\theta}_y|\mathbf{y}_j^*, \mathbf{X}_j^*) d\boldsymbol{\theta}_y.$$

Thus, given each partition of the data observations, the conditional posterior predictive density is a weighted average of the conditional predictive density with parameters drawn from baseline distribution and the cluster-wise conditional predictive density. In practice, the conditional predictive density can be approximated by averaging over S MCMC posterior samples of ρ_n , using:

$$f(y|\mathbf{y}, \mathbf{X}, \mathbf{x}) \approx \frac{1}{S} \sum_{s=1}^S \hat{f}^{(s)}(y|\mathbf{y}, \mathbf{X}, \mathbf{x}, \rho_n^{(s)}).$$

Based on the same covariate-dependent urn scheme structure, the posterior predictive expectation, conditionally on a new \mathbf{x} , is given by:

$$E(Y|\mathbf{y}, \mathbf{X}, \mathbf{x}) = \sum_{\rho_n} \left[\frac{\alpha \pi_n}{b} f_{0,\mathbf{x}}(\mathbf{x}) E_0(Y|\mathbf{x}) + \frac{1}{b} \sum_{j=1}^K n_j \pi_n f_{j,\mathbf{x}}(\mathbf{x}) E_j(Y|\mathbf{x}) \right] p(\rho_n|\mathbf{y}, \mathbf{X}),$$

where $E_0(Y|\mathbf{x})$ is the expectation of y given \mathbf{x} with distribution $f_{0,y}(y|\mathbf{x})$ and $E_j(Y|\mathbf{x})$ is the expectation of Y given \mathbf{x} with distribution $f_{j,y}(y|\mathbf{x})$. The predictive expectation can be approximated by averaging over MCMC posterior samples of ρ_n , i.e.,

$$E(Y|\mathbf{y}, \mathbf{X}, \mathbf{x}) \approx \frac{1}{S} \sum_{s=1}^S \hat{E}(Y|\mathbf{x}, \boldsymbol{\theta}_{1:n}^{(s)}),$$

where:

$$E(Y|\mathbf{x}, \boldsymbol{\theta}_{1:n}) = \frac{1}{b} \left[\alpha \int (\boldsymbol{\mu} + \mathbf{x}^T \boldsymbol{\beta}) \prod_{l=1}^p \mathcal{N}(x_l|m_l, \tau_l) G_0(d\boldsymbol{\theta}) + \sum_{j=1}^n (\boldsymbol{\mu}_{d_i} + \mathbf{x}^T \boldsymbol{\beta}_{d_i}) \prod_{l=1}^p \mathcal{N}(x_l|m_{d_i,l}, \tau_{d_i,l}) \right],$$

$$\text{and } b = \alpha \int \prod_{l=1}^p \mathcal{N}(x_l|m_l, \tau_l) G_0(d\boldsymbol{\theta}) + \sum_{i=1}^n \prod_{l=1}^p \mathcal{N}(x_l|m_{d_i,l}, \tau_{d_i,l}).$$

2.4. Posterior Consistency

Here we establish the strong posterior consistency of the NG-DPM model (1)-(2) defined by the mixture:

$$f_G(y, \mathbf{x}) = \int f(y, \mathbf{x}|\boldsymbol{\mu}, \boldsymbol{\beta}, \sigma^2, \mathbf{m}, \boldsymbol{\tau}) G(d(\boldsymbol{\mu}, \boldsymbol{\beta}, \mathbf{m}, \boldsymbol{\tau})),$$

with corresponding probability distribution P , where

$$f(y, \mathbf{x}|\boldsymbol{\mu}, \boldsymbol{\beta}, \sigma^2, \mathbf{m}, \boldsymbol{\tau}) = \mathcal{N}(y|\boldsymbol{\mu} + \mathbf{x}^T \boldsymbol{\beta}, \sigma^2) \mathcal{N}_p(\mathbf{x}|\mathbf{m}, \text{diag}(\boldsymbol{\tau}))$$

is the kernel density of the mixture, and where the model is assigned a joint prior distribution Π defined by (3), including the Dirichlet process prior for G . We denote P_0 as the true probability distribution that generates the given data set $(y_i, \mathbf{x}_i)_{i=1}^n = (\mathbf{y}, \mathbf{X})$, with corresponding true density function given by:

$$f_0(y, \mathbf{x}) = \int f(y, \mathbf{x}|\mu, \boldsymbol{\beta}, \sigma_0^2, \mathbf{m}, \boldsymbol{\tau}) G_0^*(d(\mu, \boldsymbol{\beta}, \mathbf{m}, \boldsymbol{\tau})),$$

where σ_0^2 is the true error variance and G_0^* is the true mixing distribution.

By strong posterior consistency, we mean that the prior Π gives rise to a posterior distribution which has the following convergence property at the true f_0 ,

$$\Pi_n(A_\varepsilon | (y_i, \mathbf{x}_i^T)_{i=1}^n) \rightarrow 1,$$

for any $\varepsilon > 0$, and almost surely with respect to P_0^∞ , the infinite product measure of P_0 . Also, $A_\varepsilon = \{f \in \mathbb{F} : d_H(f, f_0) < \varepsilon\}$ is a Hellinger neighborhood around f_0 , where $d_H(f, f_0) = \left\{ \int [f^{\frac{1}{2}}(y, \mathbf{x}) - f_0^{\frac{1}{2}}(y, \mathbf{x})]^2 \omega(dy \times d\mathbf{x}) \right\}^{\frac{1}{2}}$ is the Hellinger distance between f and f_0 , and \mathbb{F} is the space of probability density functions with respect to Lebesgue measure ω .

Theorem 1. *If the prior Π in (3) for the NG-DPM model assigns σ^2 an inverse-gamma distribution which puts zero probability mass around a small neighborhood of 0, and if the DP prior for G assigns weak support to G_0^* , then the posterior distribution satisfies strong consistency in the sense that for any $\varepsilon > 0$, $\Pi_n(A_\varepsilon | (y_i, \mathbf{x}_i^T)_{i=1}^n) \rightarrow 1$ almost surely with respect to P_0^∞ .*

Proof. Strong posterior consistency for the NG-DPM model is achieved by priors which satisfy $\Pi(W_{\delta, \xi} \cap A_\varepsilon^c) = 0$ (Barron et al., 1999; Walker et al., 2005), where

$$W_{\delta, \xi} = \{(\sigma^2, G) : |\sigma^2 - \sigma_0^2| < \xi, G \in W_\delta\}$$

is a weak neighborhood of the true data-generating parameters (σ_0^2, G_0^*) with $\sigma_0^2 > \xi > 0$, and

$$W_\delta = \left\{ G : \left| \int \phi_i dG - \int \phi_i dG_0^* \right| < \delta, i = 1, \dots, k \right\}$$

is a weak neighborhood around G_0^* , with respect to a k -tuple of continuous and bounded real-valued functions ϕ_i defined on Θ , the space of $(\mu, \boldsymbol{\beta}, \mathbf{m}, \boldsymbol{\tau})$. In particular, $W_{\delta, \xi} \cap A_\varepsilon^c$ is a pathological set which can give rise to posterior inconsistency (Barron et al., 1999). In the full prior (3) of the NG-DPM model, the prior distribution for σ^2 can be easily specified to assign zero mass around a small neighborhood of 0; and Dirichlet process prior distribution for G can be easily specified to support any weak neighborhood W_δ around G_0^* for all $\delta > 0$ and any G_0^* (Ferguson, 1973). As a consequence, if $(\sigma^2, G) \rightarrow (\sigma_0^2, G_0^*)$, then from:

$$\begin{aligned} & \left| \int f(y, \mathbf{x}|\mu, \boldsymbol{\beta}, \sigma^2, \mathbf{m}, \boldsymbol{\tau}) G(d(\mu, \boldsymbol{\beta}, \mathbf{m}, \boldsymbol{\tau})) - \int f(y, \mathbf{x}|\mu, \boldsymbol{\beta}, \sigma_0^2, \mathbf{m}, \boldsymbol{\tau}) G_0^*(d(\mu, \boldsymbol{\beta}, \mathbf{m}, \boldsymbol{\tau})) \right| \\ & \leq \int |f(y, \mathbf{x}|\mu, \boldsymbol{\beta}, \sigma^2, \mathbf{m}, \boldsymbol{\tau}) - f(y, \mathbf{x}|\mu, \boldsymbol{\beta}, \sigma_0^2, \mathbf{m}, \boldsymbol{\tau})| G_0^*(d(\mu, \boldsymbol{\beta}, \mathbf{m}, \boldsymbol{\tau})) \\ & + \left| \int f(y, \mathbf{x}|\mu, \boldsymbol{\beta}, \sigma^2, \mathbf{m}, \boldsymbol{\tau}) \{G(d(\mu, \boldsymbol{\beta}, \mathbf{m}, \boldsymbol{\tau})) - G_0^*(d(\mu, \boldsymbol{\beta}, \mathbf{m}, \boldsymbol{\tau}))\} \right|, \end{aligned}$$

one has that $f_G(y, \mathbf{x}) \rightarrow f_0(y, \mathbf{x})$ point-wise for all (y, \mathbf{x}) , and then Scheffé's theorem implies that $f_G \rightarrow f_0$ in total variation norm, thus in the Hellinger distance. This means that $(\sigma^2, G) \in W_{\delta, \xi}$ implies that $f_G \in A_\varepsilon$, leading to $\Pi(W_{\delta, \xi} \cap A_\varepsilon^c) = 0$. The above arguments provide extensions of a proof on posterior consistency for a univariate normal finite-mixture model (Walker et al., 2005, Section 3.2). \square

2.5. Variable Selection

The regression coefficients β 's do not have positive probabilities of taking on a value of zero in the prior or the posterior, due to the absolute continuity of the Normal-Gamma shrinkage prior. However, we may adopt the Scaled Neighborhood (SN) criterion of Li and Lin (2010) for variable selection. Specifically, for each data point and its estimated posterior cluster membership \hat{d}_i for $i = 1, \dots, n$ obtained by an optimal clustering rule (see Section 2.6), we obtain the MCMC posterior samples of coefficients matrix $\mathbf{B}_{\hat{d}_i} = (\boldsymbol{\beta}_{\hat{d}_i, 1}, \dots, \boldsymbol{\beta}_{\hat{d}_i, p})$, where $\boldsymbol{\beta}_{\hat{d}_i, l}$ (for $l = 1, \dots, p$) are S -dimensional vectors consisting of posterior samples. Then, for each $l = 1, \dots, p$, we compute the coordinate-wise (SN) posterior probability P_{il} that β_l is within the scaled neighborhood $[-\sqrt{\text{var}(\beta_{\hat{d}_i, l} | \mathbf{y}, \mathbf{X})}, \sqrt{\text{var}(\beta_{\hat{d}_i, l} | \mathbf{y}, \mathbf{X})}]$, based on marginal posterior variances estimated from the MCMC sampling algorithm. The decision of whether to exclude the l th covariate for observation i in cluster \hat{d}_i depends on whether the SN probability P_{il} exceeds a threshold p^* , usually chosen as $p^* = \frac{1}{2}$.

2.6. Clustering

In Bayesian inference, an optimal point estimator $\hat{\rho}$ of the clustering is obtained by the minimizing solution:

$$\hat{\rho} = \arg \min_{\rho'} \sum_{\rho} \mathcal{L}(\rho', \rho) \pi(\rho | \mathbf{y}, \mathbf{X}),$$

where \mathcal{L} is a chosen loss function and $\pi(\rho | \mathbf{y}, \mathbf{X})$ is the posterior distribution of the clustering partition ρ . Here, we choose the loss function $\mathcal{L}(a, z)$ by the variation of information (VI) (Meilă, 2007), which is based on information theory and is invariant to label-switching of the cluster assignments $\rho = \{d_i\}_{i=1}^n$. The VI between two clusterings (ρ', ρ) is the sum of their Shannon entropies minus twice the information they share. For clustering estimation we implemented the method of Rastelli and Friel (2018), a greedy algorithm which aims to find the minimizing solution $\hat{\rho} = \arg \min_{\rho'} \frac{1}{S} \sum_{s=1}^S \mathcal{L}(\rho', \rho_{n,s})$, based on S MCMC posterior samples of the partitions $\rho_{n,s} = \{d_{i,s}\}_{i=1}^n \sim \pi(\rho | \mathbf{y}, \mathbf{X})$ for $s = 1, \dots, S$.

3. Simulation Study

We compared the NG-DPM model and the N-DPM model, in terms of predictive, variable selection, and clustering accuracy, over 10 repetitions of various data simulation conditions differing by sample size ($n = 40, 200$, or 500), covariate dimensionality ($p = 10, 50$, or 100), and true number of clusters ($J = 4$ or 10). The N-DPM model is the standard DPM model assigned a normal baseline prior with no variable selection:

$$g_0(\mu_j, \boldsymbol{\beta}_j, \mathbf{m}_j, \boldsymbol{\tau}_j) = \text{N}_{p+1}((\mu_j, \boldsymbol{\beta}_j) | \boldsymbol{\eta}, \boldsymbol{\Sigma}) \prod_{l=1}^p \left[\text{N}(m_{lj} | m_0, \frac{\tau_{lj}}{N_0}) \text{Inv-Gamma}(\tau_{lj} | \frac{\nu_0}{2}, \frac{2}{\nu_0 s_0^2}) \right],$$

with hyperpriors $\boldsymbol{\eta} \sim N_{p+1}(\mathbf{0}, \mathbf{I}_{p+1})$ and $\boldsymbol{\Sigma} \sim \text{Wishart}(p+1, \mathbf{I}_{p+1})$. Throughout the simulations, both models assumed the prior parameter specifications $n_0 = 0.1$, $m_0 = 0$, $\nu_0 = 2$, $s_0^2 = 2$, $\alpha_0 = 2$, $\theta_0 = 2$, $\alpha_\alpha = 2$, $\theta_\alpha = 2$. For each simulated data set analyzed, both models were fitted using 5,000 MCMC sampling iterations, which typically produced samples that converged to the posterior distribution according to univariate trace plots, after excluding the 2,000 initial samples as burn-in.

Data sets were simulated based on a mixture of J -component normal mixture for (y, \mathbf{x}) , with equal mixture weights $1/J$, as follows. Each data set was simulated by drawing each data point (y_i, \mathbf{x}_i) by sampling $d_i \sim \text{DiscreteUniform}(1, J)$, $x_{il} \sim N(m_{d_i, l}, \tau_{d_i, l})$ for $l = 1, \dots, p$, and $y_i \sim N(\mu_{d_i} + \mathbf{x}_i^T \boldsymbol{\beta}_{d_i}, \sigma^2)$ for $i = 1, \dots, n$. For $j = 1, \dots, J$, $\boldsymbol{\tau}_j \equiv (1, \dots, 1)^T$, $\mathbf{m}_j = j \times (2, \dots, 2)^T$, $\mu_j = 10 - 2 \times (j - 1)$ if $j \leq 5$ else $10 - 2j$, $\boldsymbol{\beta}_j = (\underbrace{3, \dots, 3}_{6-j}, 0, \dots, 0)^T$ if $j \leq 5$ else $\boldsymbol{\beta}_j = (\underbrace{-3, \dots, -3}_{j-5}, 0, \dots, 0)^T$, and error variance $\sigma^2 = 1$.

We compared the two DPM models by computing, for each, the following criteria:

- **Prediction accuracy:** This was evaluated by $L1 = \frac{1}{n_t} \sum_{i=1}^{n_t} |y_{n+i} - E[Y_{n+i} | \mathbf{x}_{n+i}]|$ and $L2 = \frac{1}{n_t} \sum_{i=1}^{n_t} (y_{n+i} - E[Y_{n+i} | \mathbf{x}_{n+i}])^2$ error on new test data of size $n_t = 100$, simulated as above.
- **Variable selection accuracy:** This was evaluated using Average Area Under the Curve scores $\text{A-AUC} = \frac{1}{n} \sum_{i=1}^n \text{AUC}_i$ based on Receiver Operation Characteristic curve analysis. Here AUC_i was computed according to observation i 's corresponding coefficient posterior probability P_{il} (the SN probability; see Section 2.5) against its true relevant predictor label $\mathbf{1}_{(\beta_{d_i, l} \neq 0)}$ for $l = 1, \dots, p$, where $\boldsymbol{\beta}_{d_i}$ is the true regression coefficient in the cluster group d_i that sample i belongs to. The parameter estimation performances were also measured by Average Squared Error $\text{ASE} = \frac{1}{n} \sum_{i=1}^n \frac{1}{p} \|\hat{\boldsymbol{\beta}}_{\hat{d}_i}^{\text{med}} - \boldsymbol{\beta}_{d_i}\|^2$, where \hat{d}_i is i 's cluster membership index from optimal partition rule $\hat{\rho} = \{\hat{d}_1, \dots, \hat{d}_n\}$, and $\hat{\boldsymbol{\beta}}_{\hat{d}_i}^{\text{med}}$ is the posterior median of slope coefficients based on the estimated cluster group \hat{d}_i .
- **Clustering accuracy:** This was evaluated by the Rand (1971) Index, the Adjusted Rand Index (Hubert and Arabie, 1985), and the estimated number of clusters, \hat{J} .

The results of the simulation study are as follows. As shown in Table 1, the NG-DPM model generally outperformed the N-DPM in terms of prediction accuracy and ASE under various conditions defined by n , p and J , especially when the dimension p is much larger than each of the true cluster size. This seems due to the Normal-Gamma prior, which can shrink the coefficients of irrelevant covariates towards zero. In addition, both models generally performed competitively well on variable selection and clustering accuracy, due to the joint modeling on the covariates and the conditional response, which can distinguish covariate information between cluster groups. However, when the dimension p is much larger than cluster size (e.g., when $n = 200$, $p = 100$, $J = 10$), the NG-DPM model achieved much better

Condition			L1	L1	L2	L2	A-AUC	A-AUC	ASE	ASE
n	p	J	NG	N	NG	N	NG	N	NG	N
40	10	4	1.61 (0.27)	1.67 (0.30)	4.41 (1.53)	4.92 (1.88)	0.81 (0.09)	0.86 (0.05)	0.29 (0.11)	0.33 (0.13)
40	50	4	4.06 (0.28)	15.99 (2.99)	25.35 (2.38)	430.83 (154.05)	0.81 (0.07)	0.70 (0.10)	0.50 (0.03)	7.49 (2.00)
200	10	4	0.86 (0.04)	0.89 (0.05)	1.16 (0.11)	1.22 (0.11)	0.87 (0.04)	0.85 (0.03)	0.01 (0.00)	0.02 (0.01)
200	50	4	0.98 (0.14)	1.60 (0.22)	1.53 (0.39)	4.28 (1.05)	0.89 (0.04)	0.93 (0.02)	0.01 (0.00)	0.07 (0.01)
200	100	4	1.04 (0.12)	2.67 (0.39)	1.70 (0.32)	11.05 (3.49)	0.89 (0.03)	0.89 (0.02)	0.01 (0.00)	0.09 (0.01)
200	10	10	1.64 (0.66)	1.48 (0.49)	6.65 (3.85)	5.15 (3.91)	0.88 (0.05)	0.90 (0.03)	0.36 (0.31)	0.22 (0.16)
200	50	10	2.16 (1.35)	4.69 (1.67)	5.20 (1.76)	47.47 (33.11)	0.92 (0.02)	0.84 (0.08)	0.26 (0.43)	1.13 (0.95)
200	100	10	3.28 (0.89)	7.24 (2.03)	21.39 (11.96)	89.89 (49.62)	0.89 (0.02)	0.5 (0.11)	0.17 (0.04)	0.79 (0.31)
500	50	4	0.83 (0.08)	1.00 (0.01)	1.11 (0.25)	1.59 (0.35)	0.88 (0.03)	0.90 (0.03)	0.01 (0.00)	0.01 (0.00)
500	50	10	1.34 (0.33)	1.82 (0.70)	3.51 (1.58)	6.1 (5.40)	0.93 (0.02)	0.94 (0.02)	0.05 (0.02)	0.11 (0.09)
			RI	RI	ARI	ARI	\hat{J}	\hat{J}		
n	p	J	NG	N	NG	N	NG	N		
40	10	4	0.96 (0.06)	1 (0)	0.90 (0.06)	1 (0)	3.67 (0.47)	4 (0)		
40	50	4	1 (0)	0.98 (0.04)	1 (0)	0.96 (0.04)	4 (0)	3.88 (0.33)		
200	10	4	1 (0)	1 (0)	1 (0)	1 (0)	4 (0)	4 (0)		
200	50	4	1 (0)	1 (0)	1 (0)	1 (0)	4 (0)	4 (0)		
200	100	4	1 (0)	1 (0)	1 (0)	1 (0)	4 (0)	4 (0)		
200	10	10	0.98 (0.01)	0.99 (0.01)	0.92 (0.01)	0.94 (0.01)	9.20 (0.75)	9.50 (0.50)		
200	50	10	0.98 (0.01)	0.98 (0.01)	0.92 (0.01)	0.91 (0.01)	9.25 (0.66)	9.12 (0.60)		
200	100	10	0.98 (0.02)	0.98 (0.02)	0.90 (0.02)	0.89 (0.02)	9.14 (0.83)	8.86 (1.25)		
500	50	4	1 (0)	1 (0)	1 (0)	1 (0)	4 (0)	4 (0)		
500	50	10	0.98 (0.01)	0.99 (0.02)	0.90 (0.01)	0.95 (0.02)	9.00 (0.58)	9.50 (0.76)		

Table 1: For the NG-DPM and N-DPM models, mean (standard error) of predictive accuracy, variable selection accuracy, and clustering accuracy statistics, obtained over 10 replications, for each of the 10 simulation conditions.

variable selection results under high-dimensional covariate scenarios (large p), according to the A-AUC score.

4. Real Data Illustration

We illustrate the methodology through the analysis of the Diabetes data set from the LASSO literature (Gramacy, 2019). This data set contains observations of 442 medical patients on 10 baseline covariates, namely age, sex, body mass index, average blood pressure, and six blood serum measurements (10 baseline covariates named age, sex, bmi, map, tc, ldl, hdl, tch, ltg, glu); and on a dependent response variable (Y) defined by a measure of disease progression over one year after baseline. Before data analysis, the $n = 442$ data observations of each of the 10 covariates were transformed by a quadratic polynomial basis expansion, leading to the construction of $p = 64$ total covariates, including 10 main effects, 9 squares, and 45 two-way interactions. Then, the 442 observations for each of the $p = 64$ covariates were transformed to z -scores, having sample mean 0 and variance 1.

Afterwards, the NG-DPM and N-DPM models were each applied to analyze the Diabetes data on the 64 covariates and responses, using the same prior and MCMC specifications used in Section 3. Also, we computed the mean-squared predictive error for the NG-DPM model and for the N-DPM model on the data, using the criterion $L^2(m) = \sum_{i=1}^n [\{E(Y_i|\mathbf{x}_i) - y_i\}^2 + \text{var}(Y_i|\mathbf{x}_i)]$ (Laud and Ibrahim, 1995).

Our model achieved a better predictive performance ($L^2(m) = 3,568,906$) than the N-DPM ($L^2(m) = 3,818,953$). Figure 1 shows that the NG-DPM model obtained 17 clusters

among the 442 patients. Figure 2 presents the marginal posterior medians and cluster-wise variable selection results for the coefficients of the 64 covariates, based on the SN criterion using threshold $p^* = 0.50$. These results show different variable selection (sparsity) patterns across the 17 clusters. Such variable selection results can provide more insights into differences among the patients, and lead to more targeted treatments on each cluster group of patients.

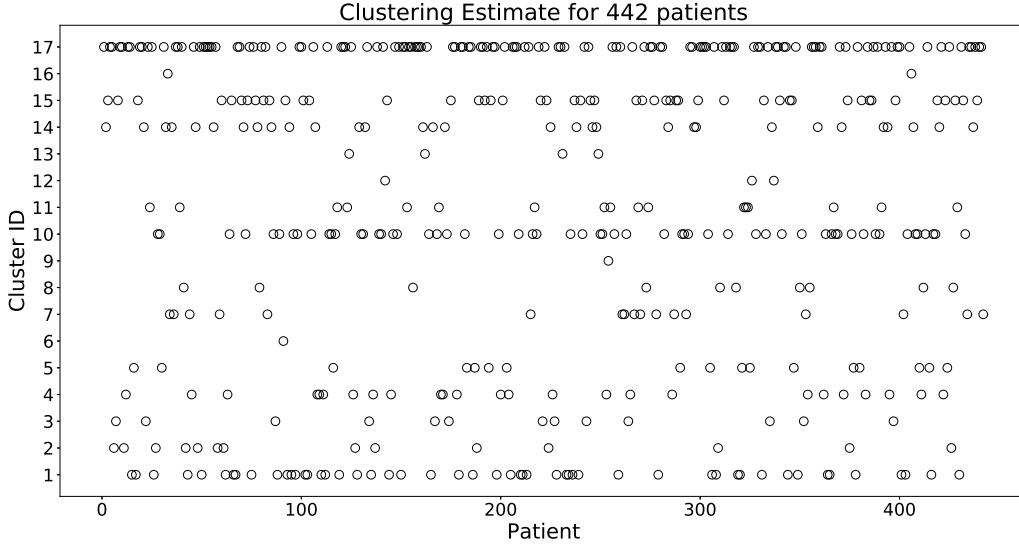


Figure 1: The clustering estimate for each of the $n = 442$ medical patients.

5. Conclusions

We proposed a novel DPM model, assigned a Normal-Gamma prior on the regression coefficients, which provides prediction and cluster-wise covariate selection, by partitioning the data based on both covariate and response information. In future research, the novel model can be extended to other nonparametric priors which generalize the DP, or to mixtures of generalized linear models.

Acknowledgments

The article represents work from the first author's Ph.D. dissertation, and is supported by National Science Foundation grant SES-1156372 awarded to the second author.

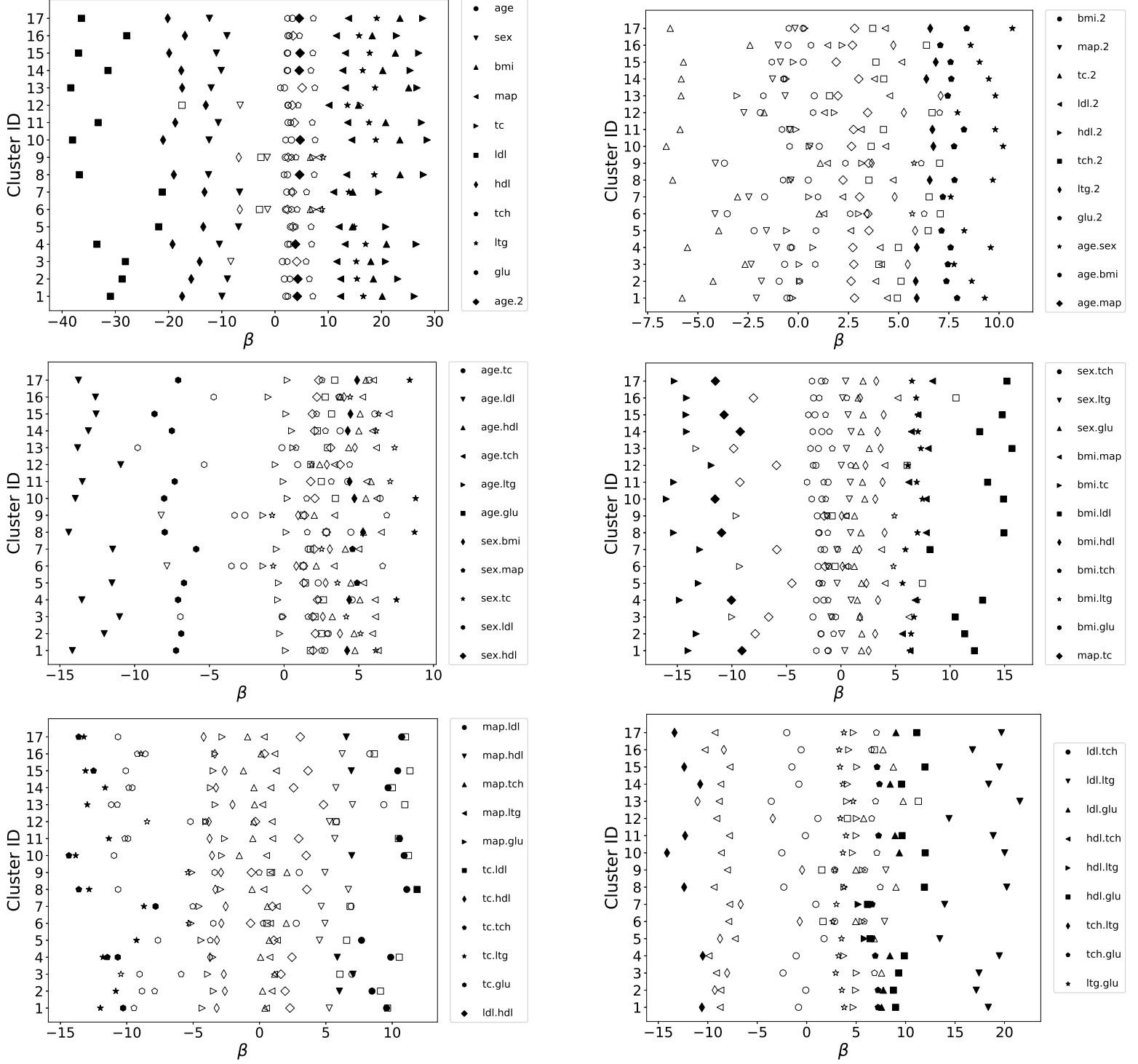


Figure 2: For the NG-DPM model, the marginal posterior medians of the 64 regression coefficients, and cluster-wise variable selection results. A filled marker indicates a significant covariate according to the SN criterion using threshold $p^* = 0.5$.

References

- Andrews, D.F., Mallows, C.L., 1974. Scale mixtures of normal distributions. *Journal of the Royal Statistical Society, Series B* 36, 99–102.
- Barcella, W., De Iorio, M., Baio, G., Malone-Lee, J., 2016. Variable selection in covariate dependent random partition models: An application to urinary tract infection. *Statistics in Medicine* 35, 1373–1389.
- Barron, A., Schervish, M.J., Wasserman, L., 1999. The consistency of posterior distributions in nonparametric problems. *Annals of Statistics* 27, 536–561.
- Castillo, I., Schmidt-Hieber, J., Van der Vaart, A., 2015. Bayesian linear regression with sparse priors. *Annals of Statistics* 43, 1986–2018.
- Escobar, M.D., West, M., 1995. Bayesian density estimation and inference using mixtures. *Journal of the American Statistical Association* 90, 577–588.
- Ferguson, T.S., 1973. A Bayesian analysis of some nonparametric problems. *Annals of Statistics* 1, 209–230.
- Gramacy, R.B., 2019. R package monomvn. R package version 1.9-13.
- Griffin, J.E., Brown, P.J., 2010. Inference with normal-gamma prior distributions in regression problems. *Bayesian Analysis* 5, 171–188.
- Hannah, L.A., Blei, D.M., Powell, W.B., 2011. Dirichlet process mixtures of generalized linear models. *Journal of Machine Learning Research* 12, 1923–1953.
- Hubert, L., Arabie, P., 1985. Comparing partitions. *Journal of Classification* 2, 193–218.
- Karabatsos, G., Walker, S.G., 2012. Bayesian nonparametric mixed random utility models. *Computational Statistics & Data Analysis* 56, 1714–1722.
- Laud, P.W., Ibrahim, J.G., 1995. Predictive model selection. *Journal of the Royal Statistical Society, Series B* 57, 247–262.
- Li, Q., Lin, N., 2010. The Bayesian elastic net. *Bayesian Analysis* 5, 151–170.
- MacEachern, S.N., 1999. Dependent nonparametric processes, in: *ASA Proceedings of the Section on Bayesian Statistical Science*, Alexandria, Virginia. Virginia: American Statistical Association; 1999. pp. 50–55.
- Meilă, M., 2007. Comparing clusterings—an information based distance. *Journal of Multivariate Analysis* 98, 873–895.
- Neal, R.M., 2003. Slice sampling. *Annals of Statistics* 31, 705–741.
- Park, T., Casella, G., 2008. The Bayesian Lasso. *Journal of the American Statistical Association* 103, 681–686.

- Quintana, F.A., Mueller, P., Jara, A., MacEachern, S.N., 2020. The dependent Dirichlet process and related models. arXiv preprint arXiv:2007.06129 .
- Quintana, F.A., Müller, P., Papoila, A.L., 2015. Cluster-specific variable selection for product partition models. *Scandinavian Journal of Statistics* 42, 1065–1077.
- Rand, W.M., 1971. Objective criteria for the evaluation of clustering methods. *Journal of the American Statistical Association* 66, 846–850.
- Rastelli, R., Friel, N., 2018. Optimal Bayesian estimators for latent variable cluster models. *Statistics and Computing* 28, 1169–1186.
- Sethuraman, J., 1994. A constructive definition of Dirichlet priors. *Statistica Sinica* 4, 639–650.
- Tibshirani, R., 1996. Regression shrinkage and selection via the lasso. *Journal of the Royal Statistical Society, Series B* 58, 267–288.
- Tibshirani, R., 2011. Regression shrinkage and selection via the lasso: A retrospective. *Journal of the Royal Statistical Society, Series B* 73, 273–282.
- Wade, S., Dunson, D.B., Petrone, S., Trippa, L., 2014a. Improving prediction from Dirichlet process mixtures via enrichment. *Journal of Machine Learning Research* 15, 1041–1071.
- Wade, S., Walker, S.G., Petrone, S., 2014b. A predictive study of Dirichlet process mixture models for curve fitting. *Scandinavian Journal of Statistics* 41, 580–605.
- Walker, S.G., Lijoi, A., Prünster, I., 2005. Data tracking and the understanding of Bayesian consistency. *Biometrika* 92, 765–778.

Appendix A. Appendix: MCMC Algorithm for the NG-DPM Model

Equation (4) gives the joint posterior distribution of the model parameters, up to a proportionality constant. The MCMC algorithm for sampling the posterior distributions is described as follows:

Step 0: Initialization: Denote s as the iteration index within MCMC algorithm. Initialize with starting values by setting $s = 0$, draw $d_i^{(0)} \sim \text{Unif}\{1, \dots, n\}$ for $i = 1, \dots, n$. Then for $j = 1, \dots, M^{(0)} = \max_i d_i^{(0)}$, $\lambda_j^{(0)} \sim \text{Exp}(1)$, $\gamma_j^{-2(0)} \sim \text{Gamma}(2, \frac{2V}{\lambda_j^{(0)}})$, where $V = \frac{1}{p} \sum_{l=1}^p \hat{\beta}_l^2 \mathbf{1}(n \geq p+1) + \frac{1}{n} \sum_{l=1}^p \tilde{\beta}_l^2 \mathbf{1}(n < p+1)$. We also initialize starting values for $\psi_{l,j}^{(0)} \sim \text{Gamma}(\lambda_j^{(0)}, 2\gamma_j^{-2(0)})$, $\mu_j^{(0)} \sim \text{N}(0, \nu_\mu)$, $\beta_j^{(0)} \sim \text{N}_p(\mathbf{0}_p, \mathbf{D}_{\psi,j}^{(0)})$, $m_{lj}^{(0)} \sim \text{N}(m_0, \tau_{lj}^{(0)}/N_0)$, $\tau_{lj}^{(0)} \sim \text{Inv-Gamma}(\frac{\nu_0}{2}, \frac{2}{\nu_0 s_0^2})$, $\sigma^{2(0)} \sim \text{Inv-Gamma}(\alpha_0, \theta_0)$, and mass parameter $\alpha^{(0)} \sim \text{Gamma}(\alpha_\alpha, \theta_\alpha)$.

Then, for each iteration $s = 1, \dots, S$, draw from the full conditional posterior distributions described in the following steps:

Step 1: Draw mixture weights $w_j^{(s)}$: For $j = 1, \dots, M^{(s)} = \max_i d_i^{(s-1)}$, take $n_j^{(s)} = \sum_{i=1}^n \mathbf{1}(d_i^{(s-1)} = j)$, $m_j^{(s)} = \sum_{i=1}^n \mathbf{1}(d_i^{(s-1)} > j)$. Then for $j = 1, \dots, M^{(s)}$, draw $v_j^{(s)} \sim \text{Beta}(1 + n_j^{(s)}, \alpha^{(s-1)} + m_j^{(s)})$, let $w_j^{(s)} = v_j^{(s)} \prod_{l < j} (1 - v_l^{(s)})$, and draw $u_i^{(s)} \sim \text{Unif}(0, w_{d_i^{(s-1)}}^{(s)})$ for $i = 1, \dots, n$. For $j = M^{(s)} + 1, \dots, N^{(s)}$, draw $v_j^{(s)} \sim \text{Beta}(1 + n_j^{(s)}, \alpha^{(s-1)} + m_j^{(s)})$ until the smallest $N^{(s)}$ is obtained such that $\sum_{j=1}^{N^{(s)}} w_j^{(s)} > \max_i (1 - u_i^{(s)})$.

Step 2: For $j = 1, \dots, M^{(s)}$, update $\lambda_j^{(s)}$, $\gamma_j^{-2(s)}$, $\psi_j^{(s)}$, $\mu_j^{(s)}$, $\beta_j^{(s)}$, $\mathbf{m}_j^{(s)}$, $\tau_j^{(s)}$:

2.1: Draw from:

$$\begin{aligned} \lambda_j^{(s)} | \psi_j^{(s-1)}, \gamma_j^{-2(s-1)} &\propto \pi(\lambda_j) \prod_{l=1}^p \pi(\psi_{l,j}^{(s-1)} | \lambda_j, \gamma_j^{-2(s-1)}) \\ &\propto \pi(\lambda_j) \left(\frac{1}{2} \gamma_j^{-2(s-1)} \right)^{p\lambda_j} [\Gamma(\lambda_j)]^{-p} \left[\prod_{l=1}^p \psi_{l,j}^{(s-1)} \right]^{\lambda_j}. \end{aligned}$$

Since the conditional posterior distribution is not in closed form, we perform a sampling update of λ_j using the stepping-out slice sampling algorithm (Neal, 2003).

2.2: Draw from:

$$\begin{aligned} \gamma_j^{-2(s)} | \lambda_j^{(s)}, \psi_j^{(s-1)} &\propto \pi(\gamma_j^{-2} | \lambda_j^{(s)}) \prod_{l=1}^p \pi(\psi_{l,j}^{(s-1)} | \lambda_j^{(s)}, \gamma_j^{-2}) \\ &\propto \text{Gamma}(\gamma_j^{-2} | 2, V/2\lambda_j^{(s)}) \prod_{l=1}^p \left[(2\gamma_j^{-2})^\lambda \exp\left\{-\frac{1}{2}\gamma_j^{-2}\psi_l\right\} \right] \\ &\sim \text{Gamma}\left(p\lambda_j^{(s)} + 2, \left[\frac{1}{2} \sum_{l=1}^p \psi_{l,j}^{(s-1)} + V/2\lambda_j^{(s)}\right]\right). \end{aligned}$$

2.3: For $l = 1, \dots, p$, draw from the Generalized Inverse Gaussian (GIG) distribution:

$$\begin{aligned} \psi_{l,j}^{(s)} | \beta_{l,j}^{(s-1)}, \lambda_j^{(s)}, \gamma_j^{-2(s)} &\propto \pi(\psi_{l,j} | \lambda_j^{(s)}, \gamma_j^{-2(s)}) \pi(\beta_{l,j}^{(s-1)} | \psi_{l,j}) \\ &\propto \psi_{l,j}^{\lambda_j^{(s)} - 1} \exp\left\{-\frac{1}{2} \gamma_j^{-2(s)} \psi_{l,j}\right\} \psi_{l,j}^{-\frac{1}{2}} \exp\left\{-\frac{1}{2 \psi_{l,j}} \beta_{l,j}^{2(s-1)}\right\} \\ &\sim \text{GIG}\left(\lambda_j^{(s)} - \frac{1}{2}, \gamma_j^{-2(s)}, \beta_{l,j}^{2(s-1)}\right). \end{aligned}$$

2.4: If $n_j > p + 1$, draw from:

$$\begin{aligned} \mu_j^{(s)}, \beta_j^{(s)} | \mathbf{D}_{\psi,j}^{(s)}, \sigma^{2(s)} &\propto \prod_{d_i^{(s-1)}=j} \text{N}(y_i | \mathbf{x}_i, \mu_j^{(s-1)}, \beta_j, \sigma^{2(s)}) \pi(\beta_j | \mathbf{D}_{\psi,j}^{(s)}) \pi(\mu_j) \\ &\sim \text{N}_{p+1}(B^{-1} \tilde{\mathbf{X}}_j^{*T} \mathbf{y}_j^*, \sigma^{2(s)} B^{-1}), \end{aligned}$$

where $B = \tilde{\mathbf{X}}_j^{*T} \tilde{\mathbf{X}}_j^* + \sigma^{2(s)} \Lambda_j^{(s)}$, $\tilde{\mathbf{X}}_j^{*T} = [\mathbf{1}_{n_j}, \mathbf{X}_j^*]$, $\Lambda_j^{(s)} = \text{diag}(0, 1/\psi_{1,j}^{(s)}, \dots, 1/\psi_{p,j}^{(s)})$. Otherwise, if $n_j \leq p + 1$, we take the singular value decomposition $\tilde{\mathbf{X}}_j^* = F^T D A^T$, and let $\hat{\theta}_{N_j} = D^{-1} F \mathbf{y}_j^*$. Then we draw from:

$$\mu_j^{(s)}, \beta_j^{(s)} | \mathbf{D}_{\psi,j}^{(s)}, \sigma^{2(s)} \sim \text{N}_{p+1}(\Psi_j^{(s)} A C^{-1} \hat{\theta}_{N_j}, \Psi_j^{(s)} - \Psi_j^{(s)} A C^{-1} A^T \Psi_j^{(s)})$$

where $\Psi_j^{(s)} = \text{diag}(\nu_\mu, \psi_{1,j}^{(s)}, \dots, \psi_{p,j}^{(s)})$, $C = \Psi_{0j} + \sigma^{2(s)} \Lambda^*$, $\Psi_{0j} = A^T \Psi_j^{(s)} A$, $\Lambda^* = D^{-2}$.

2.5: For $l = 1, \dots, p$, draw from:

$$\tau_{jl}^{(s)} \propto \prod_{d_i^{(s-1)}=j} \text{N}(x_{il} | m_{jl}^{(s-1)}, \tau_{jl}) \pi(\tau_{jl}) \sim \text{Inv-Gamma}\left(\frac{\nu^*}{2}, \frac{2}{s^{*2} \nu^*}\right),$$

where $n^* = n_0 + n_j$, $\nu^* = \nu_0 + n_j$, $\bar{x}_{n_j,l} = \frac{1}{n_j} \sum_{i=1}^{n_j} x_{il}$, and $s^{*2} = \frac{1}{\nu^*} \left[\sum_{i=1}^{n_j} (x_{il} - \bar{x}_{n_j,l})^2 + s_0^2 \nu_0 + \frac{n_0 n_j}{n^*} (\bar{x}_{n_j,l} - m_0)^2 \right]$.

2.6: For $l = 1, \dots, p$, draw from:

$$m_{jl}^{(s)} | \tau_{jl}^{(s)} \propto \prod_{d_i^{(s-1)}=j} \text{N}(x_{il} | m_{jl}, \tau_{jl}^{(s)}) \pi(m_{jl} | \tau_{jl}^{(s)}) \sim \text{N}(m^*, \frac{\tau_{jl}^{(s)}}{n^*}),$$

where $m^* = (n_j \bar{x}_{n_j,l} + n_0 m_0) / (n_j + n_0)$.

If $N^{(s)} > M^{(s)}$, then for $j = M^{(s)} + 1, \dots, N^{(s)}$, draw $\lambda_j^{(s)} \sim \text{Exp}(1)$, $\gamma_j^{-2(s)} \sim \text{Gamma}(2, V/2\lambda_j^{(s)})$, $\psi_j^{(s)} \sim \prod_{l=1}^p \text{Gamma}(\lambda_j^{(s)}, \gamma_j^{-2(s)})$, $\beta_j^{(s)} \sim \text{N}(\mathbf{0}_p, \mathbf{D}_{\psi,j}^{(s)})$, $\mu_j^{(s)} \sim \text{N}(0, \nu_\mu)$, $\tau_j^{(s)} \sim \prod_{l=1}^p \text{Inv-Gamma}(\nu_0/2, 2/\nu_0 s_0^2)$, $\mathbf{m}_j^{(s)} \sim \prod_{l=1}^p \text{N}(m_0, \tau_{jl}^{(s)}/n_0)$.

Step 3: For $i = 1, \dots, n$, sample $d_i^{(s)} = j$ with probability proportional to:

$$\mathbf{1}(w_j^{(s)} > u_i^{(s)}) \text{N}(y_i | \mu_j^{(s)} + \mathbf{x}_i^T \beta_j^{(s)}, \sigma^{2(s)}) \text{N}_p(\mathbf{x}_i | \mathbf{m}_j^{(s)}, \tau_j^{(s)}), \text{ for } j = 1, \dots, N^{(s)}.$$

Step 4: Draw from:

$$\begin{aligned} \sigma^{2(s)} | \beta_k^*, \mu_k^* &\propto \prod_{i=1}^n N(y_i | \mu_{d_i}^{(s)} + \mathbf{x}_i^T \beta_{d_i}^{(s)}, \sigma^2) \pi(\sigma^2) \\ &\sim \text{Inv-Gamma} \left(n/2 + \alpha_0, \sum_{i=1}^n (y_i - \mu_{d_i}^{(s)} - \mathbf{x}_i^T \beta_{d_i}^{(s)})^2 / 2 + \theta_0 \right). \end{aligned}$$

Step 5: Update $\alpha^{(s)}$ by drawing from a Gamma distribution with shape $\alpha_\alpha + K - \mathbf{1}(u > \{O/(1+O)\})$ and scale $\theta_\alpha - \log(\eta)$, where K is number of unique $d_i^{(s)}$'s, $\eta \sim \text{Beta}(\alpha^{(s-1)} + 1, n)$, $u \sim \text{Uniform}(0, 1)$ and $O = (\alpha_\alpha + K - 1) / (\{\theta_\alpha - \log(\eta)\}n)$ (Escobar and West, 1995).

Sampling updates from Steps 1 through 5 are repeated for a large number of iterations until the MCMC chain has displayed good mixing, according to trace plots.

The Python software code, and the R code files, provide more details about the MCMC sampling algorithm. They are included in the Github link <https://github.com/bterding/NG-DPM/tree/master>, along with the MCMC code files for the N-DPM model, and the simulated data sets and the Diabetes data set analyzed in Sections 3 and 4 of the article.